Airborne measurement of the cloud radiation budget for stratocumulus in the Japanese Cloud-Climate Study (JACCS)

A. Uchiyama and JACCS/MRI airborne observation team

Meteorological Research Institute, Tsukuba, Ibaraki 305-0052 Japan

1. Introduction

Clouds play an important role in radiative energy budget and water cycle in the earth -atmosphere system. The Japanese Cloud-Climate Study (JACCS) is a research program focusing on cloud-radiation interactions. The major scientific objectives of the JACCS program are (1) to advance our understanding of the relationship between physical parameters and radiative properties of clouds, (2) to develop advanced uses of satellite data in the cloud-climate study, and (3) to develop better parameterization of cloud and radiation processes. In order to achieve these objectives, field observations of cloud and radiation have been planed and implemented since 1991. In this field experiment, we made aircraft observation for boundary-layer clouds.

The objectives of the JACCS airborne observation are as follows,

- to develop the airborne cloud-radiation observing system,
- to advance our understanding of the relationship between cloud physical and radiative properties,
- to assess and improve the currently used remote sensing techniques for retrieving cloud-physical parameters, and
- to study the cloud structure and evolution process.

We are specially interested in the issues of the so-called anomalous absorption of the solar radiation (Stephens and Tsay 1990, Cess et al 1995, Ramanathan et al. 1995, Pilewskie and Valero 1995). In order to solve this problem, we have made aircraft observations for boundary-layer clouds over the sea.

2. Airborne cloud-radiation observing system

In the JACCS project, we have developed an airborne cloud-radiation observing system (ACROS) by using two aircraft equipped with various instruments for simultaneous measurements of clouds and radiation. One aircraft is Cessna Titan C404, and the other is Beachcraft King Air B200. The Cessna Titan C404 mounts the instruments to measure the radiation field above cloud layer and the Beachcraft King Air B200 mounts the instruments to measure the radiation field below the cloud layer and cloud micro-physical parameters (see Table 1). The radiation budget of cloud layer is measured by two kind of broad spectral band pyranometers. One measures the solar irradiance in 0.28 to 2.9 μ m region. and the other measures the solar irradiance in 0.72 to 2.9 μ m region. The solar irradiance in the visible region can be obtained by subtracting the former (total irradiance) from the latter (near Infrared irradiance). We also use a multi-channel cloud pyranometer (MCP), which was developed by Asano et al. (1995) and has a narrow spectral band width.

3. Method of aircraft observation

We make an aircraft observation by taking the following methods and strategy into consideration.

Firstly, we make a synchronized flight, using the Global Positioning System (GPS). The synchronized flight is the most important key point in our airborne observation. By the synchronized flight, we can get the collocated and simultaneous data.

We compare the net fluxes averaged along the flight path. As shown later, the divergence or convergence of radiation fluxes are changed point by point, due to the inhomogeneity of cloud field. Therefore, we only compare the averaged fluxes. The path length is about 50 to 60 km.

We make a measurement during an hour before and after the local noon, because the

Table 1 Instrumentation of ACROS for JACCS.

Quantity measured	Instrument	Characteristics	Aircraft	
			B200*	C404'
[Radiation]				
Upward/downward spectral flux	Multichannel Cloud Pyranometer (MCP)	λ=421, 500, 675, 760, 862, 938, 1080, 1225, 1650nm		◎
Upward/downward solar flux	Pyranometer EKO MS801*/K&Z CM21'	0.3μm<λ<2.9μm (WG305)	◎	◎
Upward/downward near-IR flux	Pyranometer EKO MS801*/K&Z CM21'	0.72μm<λ<2.9μm (RG715)	◎	◎
Upward/downward infrared flux	Pyrgeometer Eppley PIR	4μm<λ<50μm	◎	◎
Nadir spectral radiance	FTIR Bomen MB155	0.71μm<λ<20μm Δν>1cm^{-1}		◎
Nadir infrared radiance (radiation temp)	Minarad RST-10	9.5μm<λ<11.5μm		◎
	Barnes IT-4	9.5μm<λ<11.5μm	◎	
Nadir microwave radiance	Radiometrics WVR-1100 (MWR)	23.8Ghz, 31.4Ghz		◎
[Cloud and aerosol]				
Cloud particle size spectrum	Airborne Video-Microscope System (AVIOM)	5μm<D<500μm	◎	
	PMS FSSP-100	2μm<D<47μm	◎	
	PMS OAP-2D2-C	25μm<D<800μm	◎	
Cloud liquid water content	PMS KLWC-5	0-5g/m^3	◎	
Effective particle radius, LWC	Gerber PVM-100A	2μm<D<70μm, 0-10g/m^3	◎	
Aerosol size spectrum	PMS PCASP-100X	0.1μm<D<3μm	◎	
[Thermodynamics]				
Total air temperature	Rosemount 102 thermometer	-50C<T<150C	◎	◎
Humidity (dew point temperature)	EG&G 137-C3 hygrometer	-65C<Td<25C	◎	◎
(water vapor absorption)	AIR Lyman-α hygrometer	λ=122nm, -80C<Td<50C	◎	
3D wind field	Rosemount 858AJ gust probe		◎	
	Rosemount 1221 pressure transducer		◎	
	POS/AV ApplAnix POS/DG 310		◎	
True air speed	Rosemount 1332B pressure transducer			◎
[Others]				
Cloud morphology	Video Camera-VCR system	Forward/Downward looking	◎	◎
Pitch/roll/yaw angles	Vertical/directional gyro-system			◎
	POS/DG310 ApplAnix		◎	
Position latitude/longitude	GPS Trimble TNL-1000		◎	◎
Data acquisition	SEA DAS M200		◎	
	Prede DAS PDX-60CH			◎

*) B200: Beechcraft B200 Super King Air (Nakanihon Air Service Co., Nagoya, Japan)
') C404: Cessna 404 Titan (Nakanihon Air Service Co., Nagoya, Japan)

Table 2 Airborne Cloud Radiation Budget.

	Location	Period	Comments
Case I	East China sea	98 Feb.	Water cloud thick/thin case
Case II	East off Sanriku	98 July	Water cloud Multi-layered Narrow spectral band pyranometer
Case III	West off Kyushu	99 Jan.	Water cloud Hazy Aerosol polluted cloud
Case IV	Wakasa Bay	99 Jan.	Mixed phase Highly inhomogeneous

change of the solar zenith angle is small during this period.

As both the upper and lower aircraft observe the similar cloud field area, the two aircraft fly at the same distance away from cloud layer.

We do not change the flight level during the radiation budget measurement in order to avoid the change of environmental condition. The change of environmental condition causes the change of pyranometer body temperature, and the false signal is measured.

We make an observation over the sea, because the lower boundary is homogeneous.

We make a flight along the longitude and latitude lines. From these data, we determine the mis-alignment of pyranometers by using continuity of downward solar irradiance.

Lastly, we carefully calibrate and correct the pyranometers. The broad band pyranometers are calibrated through side-by-side comparisons with a standard pyranometer at the Meteorological Instrument Calibration Center of the Japan Meteorological Agency (JMA). The standard deviation of calibration constant transferred from the standard pyranometer is less than 0.5%. The temperature dependence of pyranometers is take into account. The corrections for the mis-alignment of pyranometer setting on the mount and inclination of aircraft attitude are made. The delay of pyranometer response is also take into account simply.

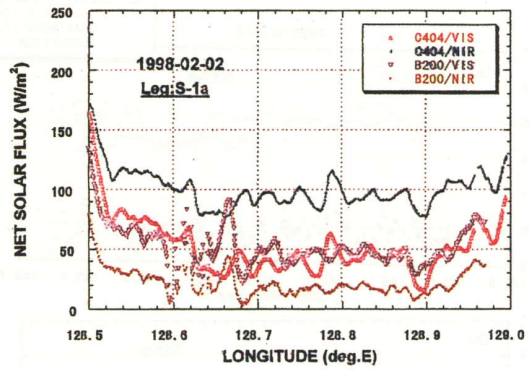

Fig. 1 Distributions of the visible and near-IR net solar fluxes measured on C404 and B200, respectively, above and below the cloud layer in longitudinal position along the S-1a leg for the stratocumulus cloud observed on 2 February 1998.

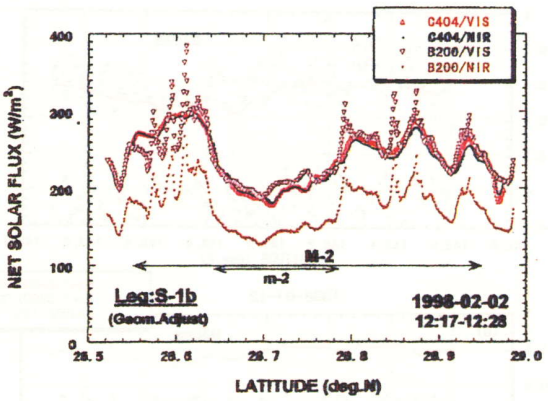

Fig. 2 Same as Fig.1 but for latitudinal distributions along the S-1b north-south leg. The B200 latitudinal position was slightly shifted to north.

4. Results

We show the four cases (Table 2). The case I, II and III are liquid water clouds. In the case II, the narrow spectral band pyranometers were used. In the case III, it was very hazy. In the case IV, the mixed phase cloud was observed.

The stratocumulus in the case I was observed in the winter season over the east China sea. The results of radiation budget for the optically thick and thin cases are shown in Fig. 1 and 2. respectively. The two lines in the middle of Fig. 1 are visible net fluxes measured on the Cessna Titan C404 and Beachcraft King Air B200. Both visible net fluxes are almost same values. This means that there is no absorption in the layer between two aircraft. In this case, the averaged absorptances are 9.3% , 19.8% and -0.2% in the total, near IR, and visible region, respectively (Table 3). The visible absorptance is nearly zero within the measurement accuracy. Assuming homogeneous cloud layer, we calculated the cloud absorptance and albedo. The cloud model assumed is based on the measurement values. The values in the blanket are calculated ones. The agreement between the measurement and calculation is good.

The net fluxes in the thin cloud case is shown in Fig. 2. Both visible net fluxes are also almost same values. The averaged absorptance are 7.6% , 15.9% and -0.3% in the total, near IR, and visible

Table 3 Solar Radiation budget due to cloud layers (case I).

[1] **Case M-1 (Thick layer)**

Averaged over Long. = 128.70～128.88° E along Leg S-1a.
θ_0 = 46.5°

	C404 DW Flux [W/m²]	C404 Net Flux [W/m²]	B200 Net Flux [W/m²]	Absorptance (%) Meas. [Calc.]	Albedo (%) Meas. [Calc.]	Cloud Model (H=1.2～2.0km)
Total	821	138	62	9.3 [10.6]	83.2 [82.9]	τ_{vis}=103
Near-IR	389	95	18	19.8 [22.3]	75 6 [73.3]	R_{eff}=8μm
Visible	432	43	44	-0.2 [0.0]	90.0 [91.2]	LWC=0.65g/m^3
						u_{H_2O}=5.5g/m^3

[2] **Case M-2 (Thin layer)**

Averaged over Lat. = 28.64～28.78° N along Leg S-1b.
θ_0 = 45.8°

	C404 DW Flux [W/m²]	C404 Net Flux [W/m²]	B200 Net Flux [W/m²]	Absorptance (%) Meas. [Calc.]	Albedo (%) Meas. [Calc.]	Cloud Model (H=1.2～1.6km)
Total	830	407	353	6.5 [8.1]	50.8 [51.7]	τ_{vis}=10
Near-IR	399	204	145	14.8 [16.4]	48.9 [47.5]	R_{eff}=7μm
Visible	431	203	208	-1.2 [0.0]	52.7 [55.6]	LWC=0.11g/m^3
						u_{H_2O}=5.5g/m^3

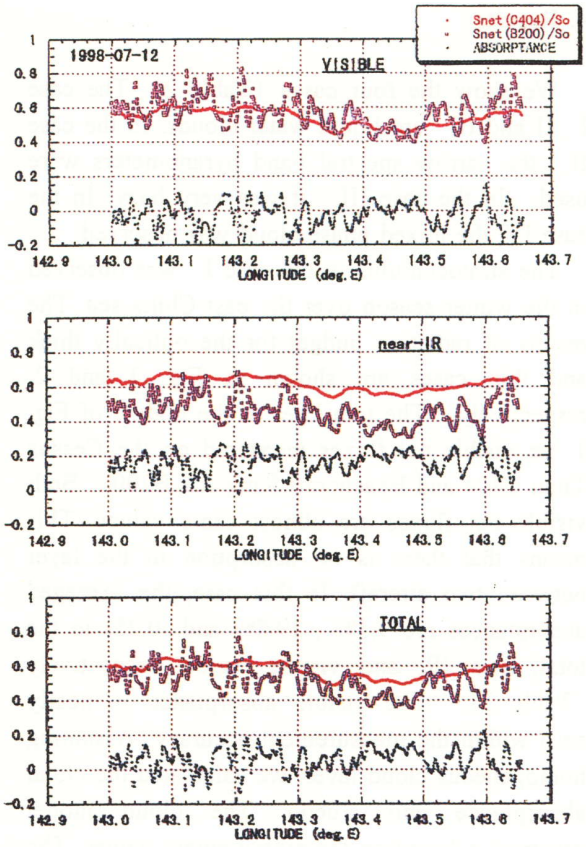

Fig. 3 Horizontal distributions, as a function of longitude, of the net solar fluxes (Snet/S0) normalized by the C404 downward solar flux measured on C404 (red) and B200 (blue) as well as the absorptance (green) for the layer between C404 and B200 altitudes in the visible (top panel), near-IR (middle panel) and total (bottom panel) band regions, respectively, for stratiformed cloud observed on 12 July 1998.

region, respectively (Table 3). The visible absorptance is also nearly zero within the measurement accuracy. The agreement between the measurement and calculation is also good.

The case I is analyzed by Asano et al. (2000) in more detail.

The stratocumulus in the case II was observed in the summer season over the east off Sanriku. In the winter season, the stratocumulus frequently includes ice particles. Therefore, we make a measurement in the summer. Furthermore, in the case II, we use the narrow spectral band pyranometer (MCP). In the Fig. 3, the results of broad band pyranometers are shown. The net fluxes are divided by the downward fluxes at the level of the Cessna Titan C404. The green dots are absorptance. In this case, the averaged

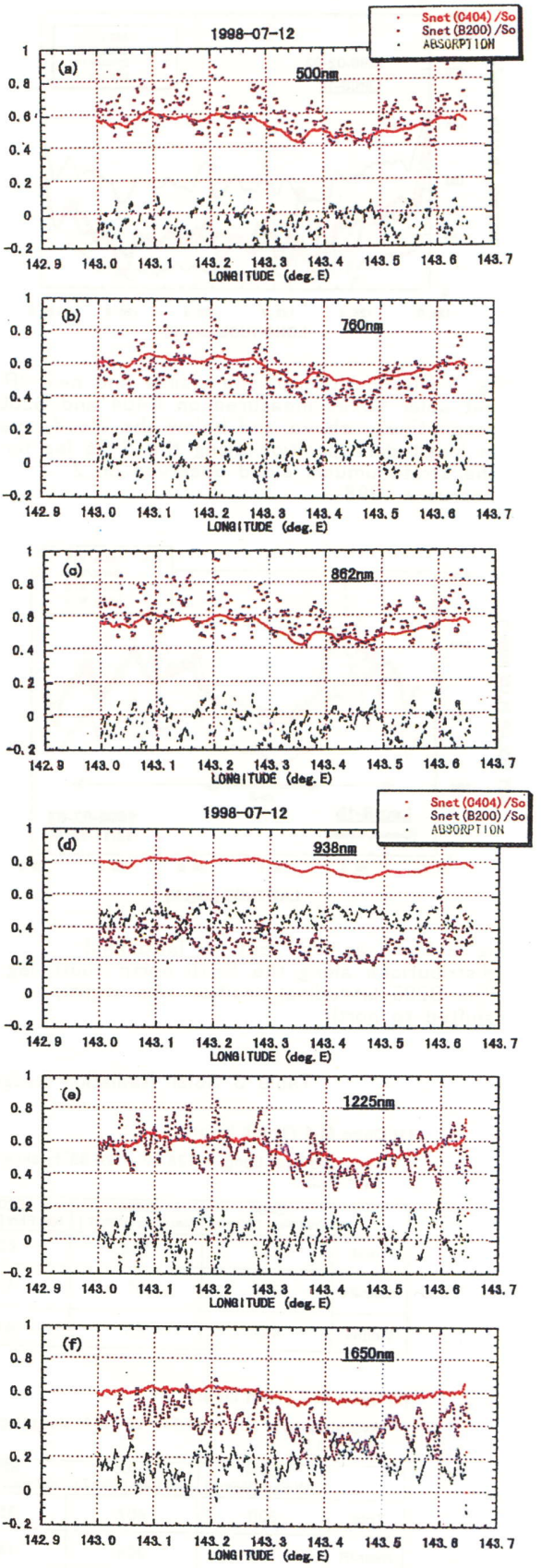

Fig. 4 Same as Fig. 3, but for wavelengths at (a)500nm,(b)760nm,(c)862nm,(d)938nm,(e)1225nm, and (f)1650nm.

Table 4 Solar radiation absorptances averaged over each flight leg for the stratiform water clouds observed on 12 and 18 July 1998 (case II).

	Visible	Near IR	Total	500nm	760nm	862nm	938nm	1225nm	1665nm
12 July path2	-0.027	0.161	0.060	-0.051	0.054	-0.057	0.467	0.025	0.178
12 July path3	0.011	0.231	0.114	-0.011	0.132	-0.012	0.601	0.061	0.232
18 July path2	-0.004	0.188	0.087	-0.003	0.061	-0.023	0.486	0.030	0.199
18 July path4	0.014	0.216	0.110	0.013	0.084	0.004	0.494	0.077	0.268

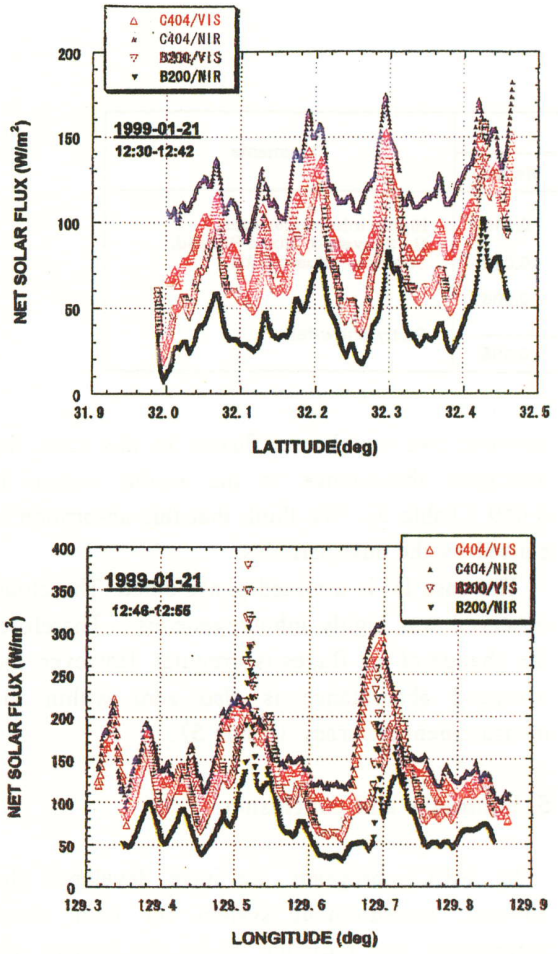

Fig. 5 Distributions, as a function of latitude (top panel) and longitude (bottom panel) along each flight leg, of the visible (VIS) and near-IR (NIR) net solar fluxes measured on C404 and B200, respectively, above and below the stratocumulus cloud observed on 21 January 1999 (case III).

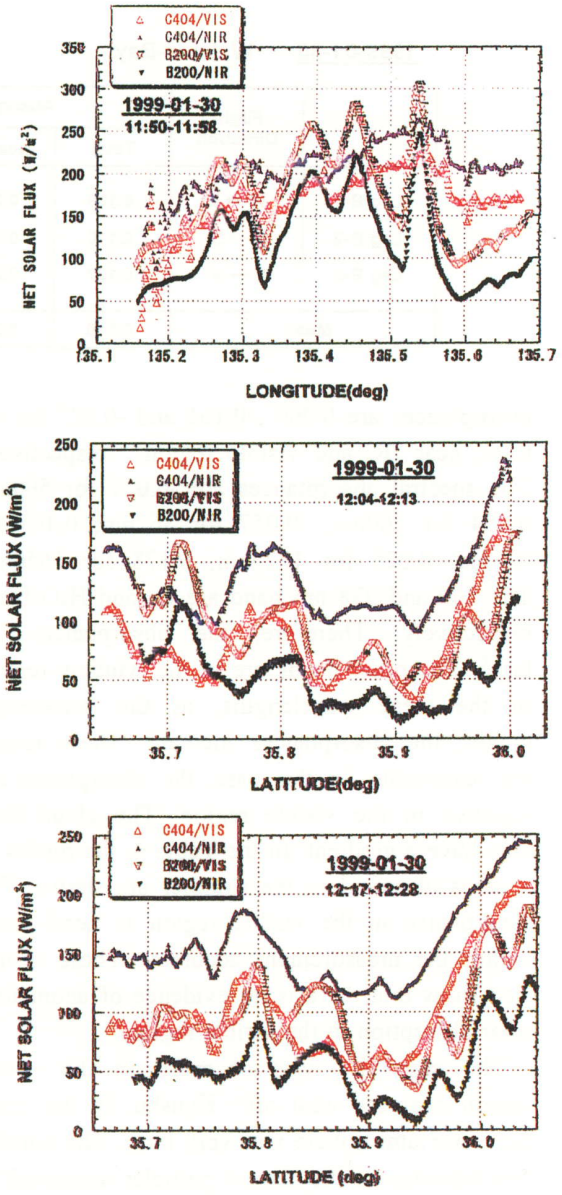

Fig. 6 Same as Fig. 5, but for the mixed-phase cloud observed on 30 January 1999 (case IV).

Table 5 Broad band solar absorptances averaged over each flight leg for the stratocumulus and mixed-phase clouds observed respectively on 21 and 30 January 1999 (case III and case IV).

1999-01-21 West off Kyushu

	Flight Direction	Absorptance			Comments
		Total	Near-IR	Visible	
Leg B-1	S → N	0.133	0.206	0.059	Super-cooled Stratocumulus
Leg B-2	W → E	0.157	0.230	0.082	Hazy
Mean		0.145	0.218	0.070	

1999-01-30 Wakasa-Bay

	Flight Direction	Absorptance			Comments
		Total	Near-IR	Visible	
Leg B-1	W → E	0.109	0.224	- 0.010	Highly inhomogeneous Multi-layered, Mixed-Phased, Stratocumulus clouds
Leg B-2	N → S	0.110	0.230	- 0.012	
Leg B-3	S → N	0.137	0.260	0.008	Partly snow-fall
Mean		0.119	0.238	- 0.005	

absorptances are 0.060 , 0.161 and -0.027 for the total, near IR, and visible region, respectively. The spectral absorptances are -0.051 for 500nm, 0.054 for 760nm, -0.057 for 862nm, 0.467 for 938nm, 0.025 for 1225nm, 0.178 for 1650nm. The 760 and 938 nm band are O_2 and H_2O band, respectively. Therefore, the absorptances are large. The other bands are in the window region. In the these wavelengths, as the wavelength longer, the absorptances increase. These results are reasonable. In this case, the absorptance are negative in the visible region. The cloud field may have a gradient. In the Table 4, the results of 4 cases observed in the summer are shown. The absorptance in the visible region is nearly zero within the measurement accuracy. These results also show that there is no evidence of anomalous solar absorption in the visible region.

The case III was observed in the winter season over the west off Kyushu. In this case, the lower atmosphere was very hazy. The number concentration of the aerosol particles measured by the PCASP in this case is twice to three times as high as in the usual case. The two lines in the middle of Fig. 5 are visible net fluxes measured on the Cessna Titan C404 and the Beachcraft King Air B200. There is systematic difference between two visible net fluxes. In this case, the averaged absorptance in the visible region is 0.059 (Table 5). We think that this absorption is caused by the dust particles.

The case IV is a mixed phase cloud. The cloud observed was highly inhomogeneous. Therefore, the change of net fluxes is irregular. However, the averaged absorptance is also zero within the measurement accuracy (Table 5).

5. Summary and conclusion

In JACCS program, we have developed the airborne measurement system for both cloud parameters and radiation. Using this system, we investigated the radiation budget of stratocumulus in the boundary layer. We made a synchronized flight, using the GPS and could obtain the collocated and simultaneous data for the both aircraft. We carefully analyzed the solar radiation budget data and obtained the following results. Firstly, there is no evidence of the so-called anomalous solar absorption for the both water and mixed phase stratocumulus clouds in the usual maritime condition. Secondly, there is detectable solar absorption in the visible region for the stratocumulus in the condition of airmass polluted

by aerosol.

We have shown the only a comparison between the measurement and calculation. Because, the cloud structure is highly inhomogeneous both horizontally and vertically. The measurement of clouds by using the aircraft is limited. Therefore, it is very difficult to make a model of cloud structure for the calculation. The Cloud Profiling Radar (CPR) is very effective instrument to observe the 3 dimensional structure of clouds. The CPR is a necessary instrument in the future study on the cloud radiative property.

Acknowledgments

JACCS is supported by the Science and Technology Agency of the Japanese government. We thank Nakanihon Air Service Co., LTD for the help with the JACCS aircraft experiment.

References

Asano, S., M. Shiobara, and Y. Nakanishi, and Y. Miyake, 1995: A multichannel cloud pyranometer system for airborne solar spectral reflectance measurements for stratocumulus clouds. *J. Atmos.Sci.*, **52**, 3556-3576.

Asano, S., A. Uchiyama, Y. Mano, M. Murakami, and Y. Takayama, 2000: No evidence for solar absorption anomaly by marine water clouds through collocated aircraft radiation measurements, *J. Geophs. Res.* (in print).

Cess, R.D., M.H. Zhang, P. Minnis, L.Corsetti, E.G. Dutton, B.W. Forgan, D.P. Garber, W.L. Gates, J.J. Hack, E.F. Harrison, X. Jing, J.T. Kiehl, C.N. Long, J.-J. Morcrette, G.L. Potter, V. Ramanathan, B. Subasilar, C.H. Whitlock, D.F. Young, and Y. Zhou, 1995: Absorption of solar radiation by clouds: Observations versus models, *Science*, **267**, 496-499, 1995.

Pilewskie, P., and F.P.J. Valero, 1995: Direct observations of excess solar absorption by clouds, *Science*, **267**, 1626-1629.

Ramanathan, V., B. Subasilar, G.J. Zhang, W. Conant, R.D. Cess, J.T. Kiehl, H.Grassl, and L. Shi, 1995: Warm pool heat budget and shortwave cloud forcing: A missing physics? *Science*, **267**, 4999-503.

Stephens, G.L., and S.-C. Tsay: On the cloud absorption anomaly, 1990: *Quart. Roy. Meteor. Soc.*, **116**, 671-704.